ATLANTIS PRESS

Advances in Engineering Research, volume 187

Third International Conference on Sustainable Innovation 2019 – Technology and Engineering (IcoSITE 2019)

Finite Element Analysis of Flexural Failure of High-Strength Reinforced Concrete Columns

1st Harun Alrasyid
Civil Engineering Departement
Institut Teknologi Sepuluh Nopember
Surabaya, Indonesia
harun@ce.its.ac.id

2nd Muhammad A Rofiq
Civil Engineering Departement
Institut Teknologi Sepuluh Nopember
Surabaya, Indonesia
rofiq.raharja@gmail.com

3rd Data Iranata
Civil Engineering Departement
Institut Teknologi Sepuluh Nopember
Surabaya, Indonesia
Iranata80@gmail.com

***Abstract*— In high-rise buildings, the column has a vital role in resisting gravity and earthquake load. The utilization of high-strength concrete and high-strength steel rebar in high-rise buildings can reduce column dimension at lower storeys. In this study, Nonlinear Finite Element was carried out to model the flexure behavior of high-strength reinforced concrete columns subjected to displacement-controlled monotonic loading and constant axial loading. Two concrete columns specimen were modeled using a 3D finite-element analysis. Two-level of axial compression load was applied, as representative of low and high axial load columns in high-rise buildings, respectively. The columns were utilized with high-strength longitudinal reinforcement, high–strength transverse reinforcement, and high concrete compressive strength. Finite element analysis was carried out with appropriate material constitutive concrete and steel, geometric modeling and mesh. The finite element analysis result showed that the prediction of force – drift relationship curves is relatively similar to the experimental result.**

Keywords—concrete column, high-strength reinforced concrete, finite element analysis

I. INTRODUCTION

Reinforced concrete materials are commonly used in buildings. They provide several advantages, such as fire-resistance, higher stiffness, and cheap cost construction. However, the utilization of normal strength of concrete and steel rebar in high rise buildings can result in larger column dimension size and severe steel congestion. Thus, the availability of area at lower storeys will be reduced. This issue can be dealt with using high-strength materials. The application of high-strength concrete and high-strength steel in columns at lower storeys of high-rise buildings lead to increases available floor area.

In this study, the material specification for high strength-steel longitudinal and transversal are SD685 (f_y= 685 MPa) and SD785 (f_y =785 MPa), respectively. The nominal strength for high-strength concrete is 70MPa. The SD685 and SD 785 rebar were originally developed in Japan and modified slightly in Taiwan by TCI New High-Strength Reinforced Concrete Committee [1]. Experimental study using high strength concrete and high strength steel on reinforced concrete columns was performed by Hwang et al. [2], Ou and Kurniawan [3,4], Ou et al. [5], and Liao et al. [6]. All these experimental researches studied the behavior of high-strength reinforced concrete columns subjected to flexure and shear behavior. However, modeling high-strength reinforced concrete columns using finite element analysis to predict its behavior has not been conducted. Completing the experimental data with additional information from finite element analysis can reduce the experimental cost.

In this study, the experimental data from Ou et al. [5] are used as models to observe the flexure behavior of high-strength reinforced concrete columns with finite element analysis. Two monoliths and four precast high-strength of reinforced concrete columns were tested under displacement-controlled double-cyclic loading and constant axial loading. Only two monoliths columns, described as CH10 and CH33, were used as the model for finite element analysis in this study. These columns have flexure failure behavior. The method and result of analysis are described in the research. The objective of this paper is to predict the flexural failure of high-strength reinforced concrete columns by using finite element analysis.

II. METHOD

The research method begins with preparing data from experiments result of high-strength reinforced concrete columns. The experimental data of two monolith high-strength reinforced concrete columns from Ou et al. [5], described as CH10 and CH33, are used in this study. These columns were used as models to be predicted with finite element analysis. The finite element analysis uses an in-house three-dimensional non-linear finite element analysis (3D-NLFEA) program developed by Piscesa et al. [7]. The models were built using SALOME [8], and the output viewed using ParaView [9]. In the analysis, the loading scheme is presented as a combination of constant axial load and monotonic displacement.

A. Column Specimen

Two monolith high-strength reinforced concrete columns of Ou, et al. [5] are defined as CH10 and CH33. The nomenclature of "CH" is defined as monolith high-strength reinforced concrete columns. The notations "10" and "33" denote axial loads of $0.1\ A_g f'_c$ and $0.33\ A_g f'_c$, respectively. The axial loads of $0.1\ A_g f'_c$ and $0.33\ A_g f'_c$ are described as low axial load and high axial load, respectively. All specimens were designed using 16 D25 for longitudinal reinforcement. The CH10 and CH33 specimens use 13mm and 16mm

diameter rebar for transverse reinforcement, respectively. The transverse reinforcement ratios for CH10 and CH33 are 2.12% and 3.20%, respectively. All columns' geometry had a typical cross-sectional dimension of 600mm x 600mm with a column height of 1800mm. The concrete covers of CH10 and CH33 were 43mm and 41mm, respectively. The specimens were installed with concrete blocks at the top and bottom ends. Specimen Geometry and details are shown in Table I, while column details are defined in Fig. 1 and Fig. 2.

TABLE I. SPECIMEN GEOMETRY AND DETAILING

Property	CH10	CH33
Height of Column (mm)	1800	1800
Width x-axis (concrete) (mm)	600	600
Width y-axis (concrete) (mm)	600	600
Concrete cover thickness (mm)	43	41
Longitudinal reinforcing bar diameter (mm)	16 D 25	
Transversal reinforcing bar diameter (mm)	13	16
Longitudinal reinforcing bar spacing (mm)	114	112
Tie pitch spacing (mm)	100	100

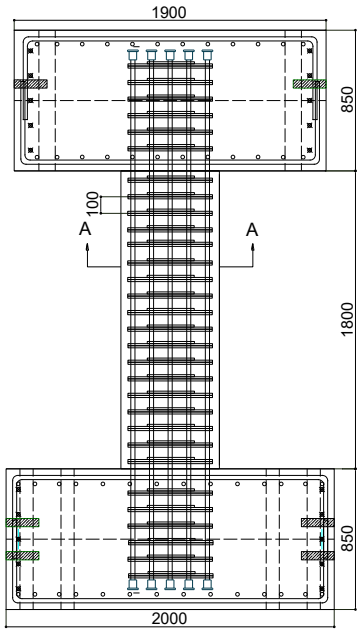

Fig. 1. Specimen Detailing

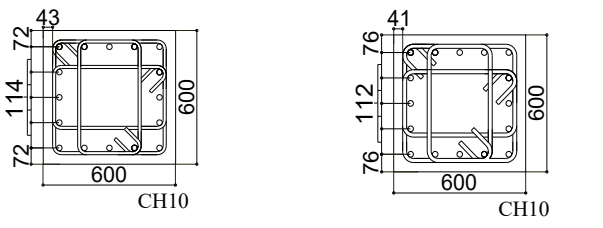

Longitudinal Bar : 16 D 25
Tranverse Bar : D13@100

Longitudinal Bar : 16 D 25
Tranverse Bar : D13@100

Fig. 2. Cross-Section

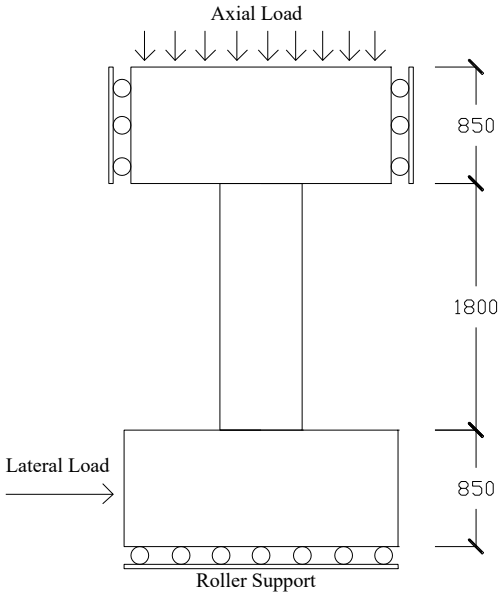

Fig. 3. Loading scheme and boundary conditions

The CH10 and CH33 utilized high-strength SD685 longitudinal steel reinforcement and SD785 transverse steel reinforcement. The actual concrete compressive strength of CH10 and CH33 are 7 MPa and 75MPa, respectively. The measured material property was obtained from the average of three samples for steel rebar and concrete. Details of the actual material test data for each specimen are shown in Table II.

TABLE II. SPECIMEN GEOMETRY AND DETAILING

Property	CH10	CH33
Concrete	f'_c= 74 MPa	f'_c= 75 MPa
Longitudinal Reinforcing Bar SD685	f_y= 713 MPa	f_y= 713 MPa
	f_u= 932 MPa	f_u= 932 MPa
Transversal Reinforcing Bar SD785	f_y= 886 MPa	f_y= 836 MPa
	f_u= 1095 MPa	f_u= 1095 MPa

B. Material Constitutive

In order to perform finite element analysis, several inputs of material properties of concrete and steel are required. Compressive strength, modulus elasticity, and Poisson ratio of concrete are involved for the concrete material property. The stress-strain relationship, modulus elasticity, and Poisson ratio are needed for steel material property. Modulus elasticity of concrete was 34140 MPa and modulus elasticity of the longitudinal and transverse rebar was 200000MPa.

In order to conduct the numerical analysis, the constitutive models for concrete and steel are required. The constitutive model of concrete compressive stress and concrete failure surface is based on Piscesa et al. [10]. The softening function under compression uses a power function [11] and is a function of the plastic dilation rate at the inflection point of the softening curve.

The constitutive for steel reinforcing bar used elastic perfectly plastic for both tension and compression. No strain hardening occurs in this assumption. This steel constitutive material is applied for both SD685 longitudinal bar and SD785 transverse bar, respectively.

C. Loading

All specimens were subjected to a combination of constant axial compression loads and monotonic displacement load. An axial compression load was put on the entire surface of the steel plate and that placed on top of concrete block, as shown in Figure 3. The axial compression loads applied for CH10 and CH33 were $0.1\ A_g f'_c$ and $0.33\ A_g f'_c$, respectively. When the axial compression load was applied continually, the horizontal displacement loads were added in the form of an impulse to a certain distance and acting monotonically. The lateral displacement load was applied on the entire surface of the side of the bottom concrete block.

The number of axial load steps is defined every second for ten seconds, while the number of lateral displacement load steps is defined every 0.1-millimeter displacement. Convergence is obtained by solving several sub-iterations in each step of the load. The accuracy of the model solution can be improved by the number of sub-iterations. Each sub-iteration has several stages until it finds a solution. Too many sub-steps can be time-consuming. Reducing the sub-steps can avoid the computational time problem. The analysis was stopped when the compressive strength of concrete reached ultimate strain, and the steel reinforcement attained rupture. The analysis process stopped when computing did not reach convergence.

D. Boundary Conditions

The boundary conditions used in modeling all column specimens are roller support, which allows for one-way translation, placed at the bottom end of the concrete block and on both sides of the concrete block. Roll supports were applied at the bottom end and both sides of the concrete block in order to permit only vertical displacements. This scheme of boundary conditions is shown in Fig. 3.

E. Numerical Analysis

The specimen models of CH10 and CH33 are built using SALOME 8.3.0 [10]. The models are shown in Figure 4. The concrete is modeled using a solid 8-noded hexahedral element with gauss point. The solid elements of concrete are separated into two parts which is the cover and core concrete of the column to consider the effect of concrete spalling. The solid models were divided into small cubical elements as shown in Figure 4(a). The steel of the longitudinal and transversal reinforcing bars is modeled using the wire element. Wire elements used in this modeling mean the reinforcing bar is defined as an element of steel wire with two degrees of freedom in each node. Two-node truss elements with exact integration were used for reinforcing bar modeling. Longitudinal and transverse reinforcing bars were modeled as one-dimensional wire elements embedded into three dimensional solid elements. The rebar nodes were perfectly bonded to concrete. This mesh configuration on numerical modeling uses 3D elements with a maximum size of 50 available in SALOME [8], as shown in Figure 5(b). The solid algorithm of mesh consists of three mesh type. The 3D and 2D elements use hexahedron and quadrangle algorithm, respectively, while the 1D element uses wire discretization algorithm available in SALOME [8]. Both column specimens are meshed with a similar pattern.

After geometry modeling is complete, then it is necessary to define the constitutive material and boundary conditions. Then the model was analyzed using an in-house three-dimensional non-linear finite element analysis (3D-NLFEA) program developed by Piscesa et al. [7]. One of the steps in finite element analysis is implementing the constitutive material. A total of 41092 nodal and 38202 eight-node hexahedral elements were used in CH10 and CH33 column specimens. These numbers were obtained to provide a convergence result. The results of the 3D-NLFEA analysis can be seen using Paraview [11].

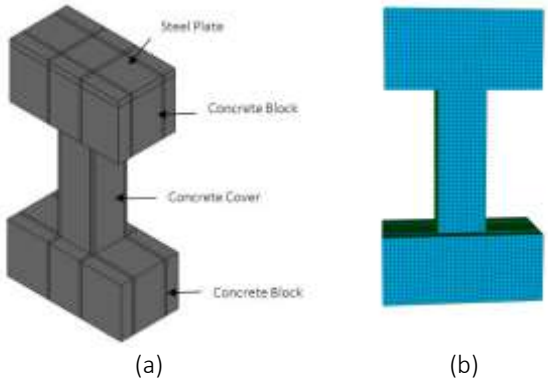

Fig. 4. The geometry of concrete (a) and meshing (b) using Salome 8.3.0

III. Result and Discussion

In this part, the result of 3D-NLFEA analysis is evaluated with the experimental result. The average envelope response of CH10 and CH33 from experimental data are compared with the monotonic response from 3D-NLFEA. This comparison can be seen in Fig. 5 and Fig. 6. The deformed column shape of CH10 at 3% nominal drift is shown in Fig. 7. Fig. 8 presents the deformed shape of CH33 at 0.75% nominal drift.

For column CH10, the prediction of force-drift relationship from the analysis is adequately accurate. The experimental result showed that the peak applied load of CH10 occurred at 1.77% actual drift with a force of 2152 KN. The 3D-NLFEA of CH10 also exhibited a similar result where the maximum force was recorded at 1.77% drift with a force of 2159 KN. The post-peak behavior prediction from 3D-NLFEA is slightly alike. The occurrence of yielding of longitudinal reinforcement between experimental data and 3d-NLFEA is at 0.62% and 0.68% actual drift, respectively. Hardening parameter and reinforcing bar stress of low axial column are presented in Fig. 7. The degree to which the elements were damaged is shown from the hardening parameter. When the hardening parameter value exceeds one, it indicates that the concrete has started to crush. Based on Fig. 7 and Fig. 8, the concrete has started to crush on the corner of column connection to concrete block. In this part, the concrete crush is due to the confining pressure of the concrete. Based on Fig. 7, confining pressure of concrete that occurs at the 3% actual drift causes the yielding on the transverse rebar. All these results show that the prediction of the flexural failure behavior of columns under combination

of low axial compression load and monotonic displacement with 3D-NLFEA show a good result.

The experimental result showed that the peak applied load of CH33 occurred at 2.80% actual drift with a force of 2852 KN. The 3D-NLFEA of CH33 predicted higher result where the maximum force recorded at 2.80% drift with a force of 3296 KN. The drift prediction from 3D-NLFEA of CH33 is greater than the results of the experiment. This may happen because of the bond-slip effect between the concrete and rebar was not considered in this analysis. It is assumed that the rebar nodes were perfectly bonded to concrete.

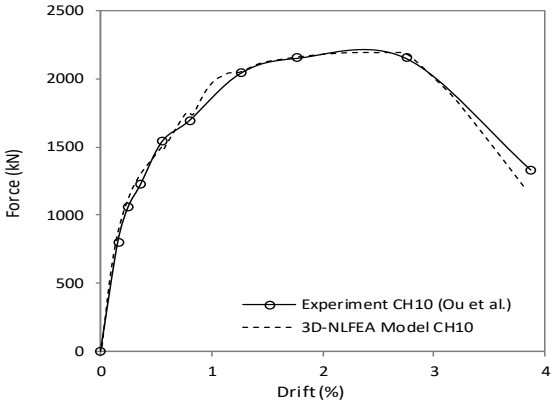

Fig. 5. Comparison force-displacement relationship from test result and 3D-NLFEA of CH10

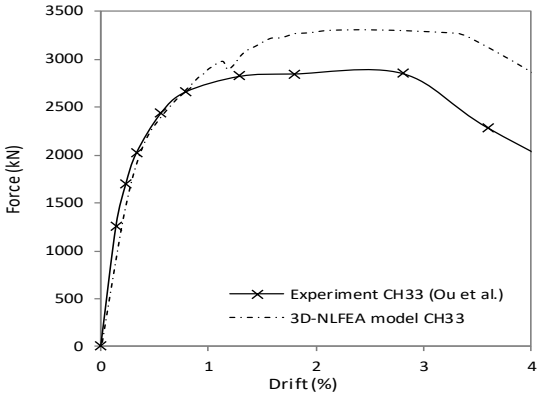

Fig. 6. Comparison force-displacement relationship from test result and 3D-NLFEA of CH33

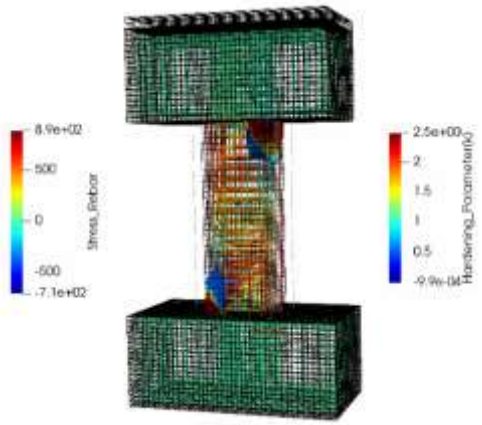

Fig. 7. Hardening parameter CH10 at 3% drift

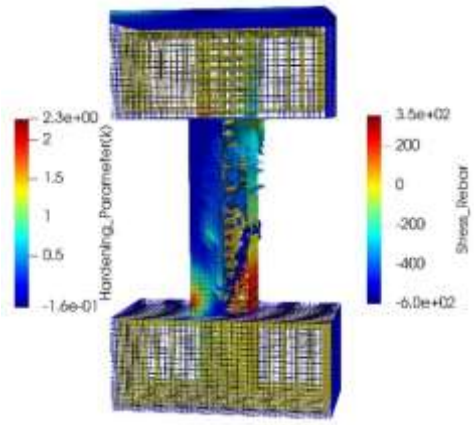

Fig. 8. Hardening parameter CH33 at 3% drift

IV. Conclusions

The paper investigates the behavior of the flexural failure of high strength concrete reinforced columns under constant axial and monotonic displacement load. The result of analysis showed that 3D-NLFEA is capable of predicting the actual force-drift relationship of high strength reinforced concrete column, particularly subjected to low axial compression load (CH10). The comparison of force drift relationship shows good agreement.

For a column with high axial compression load (CH33) the prediction of 3D-NLFEA is slightly higher. This is due to the bond-slip effect not being considered in this analysis since the rebar nodes were assumed perfectly bonded to concrete.

References

[1] TCI New High-Strength Reinforced Concrete Committee, *Steel Bars for Concrete Reinforcement -SD550W, SD685,SD685*. Taipei, Taiwan: Taiwan Concrete Institute (TCI), 2014.

[2] S. J. Hwang, G. J. Hwang, F. C. Chang, Y. C. Chen, and K. C. Lin, "Design of Seismic Confinement of Reinforced Concrete Columns Using High Strength Materials," presented at the Reinforced Concrete Columns with High Strength Concrete and Steel Reinforcement (SP-293), Toronto, Canada, 2013.

[3] Y. C. Ou and D. P. Kurniawan, "Shear Behavior of Reinforced Concrete Columns With High-Strength Steel and Concrete.," *ACI Structural Journal,* vol. 112, pp. 35-45, 2015a.

[4] Y. C. Ou and D. P. Kurniawan, "Effect of Axial Compression on Shear Behavior of High-Strength Reinforced Concrete Columns.," *ACI Structural Journal,* vol. 112, pp. 209-220, 2015b.

[5] Y. C. Ou, H. Alrasyid, Z. B. Haber, and H. J. Lee, "Cyclic Behavior of Precast High-Strength Reinforced Concrete Columns," *ACI Structural Journal,* vol. 112, pp. 839-850, 2015.

[6] W. C. Liao, W. Perceka, and M. Wang, "Experimental study of cyclic behavior of high-strength reinforced concrete columns with different transverse reinforcement detailing configurations," *Engineering Structures,* vol. 153, pp. 290-301, 2017.

[7] B. Piscesa, M. M. Attard, and A. K. Samani, "Three-Dimensional Finite Element Analysis Of Circular Reinforced Concrete Columns Confined with FRP using Plasticy Model," *Procedia Engineering,* vol. 171, pp. 847 - 856, 2017.

[8] CEA/DEN, EDF R&D, and O. CASCADE, *SALOME: The Open Source Integration Platform for Numerical Simulation ver 7.8.0*, 2016.

[9] U. Ayachit, *The ParaView Guide Community Edition*. USA: Kitware Inc., 2019.

[10] B. Piscesa, M. M. Attard, A. K. Samani, and S. Tangaramvong, "Plasticity Constitutive Model for Stress-Strain Relationship of Confined Concrete," *ACI Structural Journal,* vol. 114, pp. 361 - 371, 2017.

[11] A. K. Samani and M. M. Attard, "Lateral Strain Model for Concrete under Compression," *ACI Structural Journal,* vol. 111, pp. 441-451, 2014.